

**UCLA**

**UCLA Electronic Theses and Dissertations**

**Title**

A study of in cis versus in trans viral RNA replication: RNA molecules competing to be replicated by an RNA replicase protein

**Permalink**

<https://escholarship.org/uc/item/6nq263tq>

**Author**

Joyner, Emily

**Publication Date**

2022

Peer reviewed|Thesis/dissertation

UNIVERSITY OF CALIFORNIA

Los Angeles

A study of *in cis* versus *in trans* viral RNA replication:

RNA molecules competing to be replicated by an RNA replicase protein

A thesis submitted in partial satisfaction of the  
requirements for the degree Master of Science  
in Biochemistry, Molecular and Structural Biology

by

Emily JoAnn Joyner

2022



## ABSTRACT OF THE THESIS

A study of *in cis* versus *in trans* viral RNA replication:  
RNA molecules competing to be replicated by an RNA replicase protein

by

Emily JoAnn Joyner

Master of Science in Biochemistry, Molecular and Structural Biology

University of California, Los Angeles, 2022

Professor William M. Gelbart, Chair

A virus has one main goal: to replicate itself. To achieve this goal, many kinds of viruses must encode their own replication machinery to amplify their genomes in the host cell. This study focuses on a simple, positive-sense, single-stranded RNA virus, Nodamura, which has a genome consisting of two mRNA molecules. The translation product of RNA1 is an RNA-dependent RNA polymerase (RdRp), while its RNA2 codes for the capsid protein (CP); the RdRp binds to and replicates each of these molecules, and the CP packages the two of them into a single capsid. The focus of the current study is to assess the relative levels at which these two viral RNA molecules compete to be bound and replicated by the RdRp. Understanding replication phenomena such as this has important implications in numerous other many-molecule-mRNA-genome virus infection scenarios, in addition to potential translational medicine applications

where it is useful to amplify therapeutic mRNAs using an RdRp. In vitro transcribed Nodamura RNA constructs were created in which a fluorescent reporter gene is added to RNA1, and the CP gene in RNA2 is replaced entirely by a different fluorescent reporter. These two constructs were then transfected into mammalian (BHK-21) cells. Fluorescence intensity assays and quantitative PCR experiments were performed at various time points post-transfection to study the replication competition between Nodamura's RNA1 and RNA2 in the absence and presence of one another. These assays showed that Nodamura RNA1 replication decreases by as much as a factor of two when in the presence of RNA2, while RNA2 is not amplified at all in the presence of the RdRp encoded by RNA1. These results indicate how *in cis* and *in trans* replication dynamics determine the differential expression of the viral genomic RNAs.

The thesis of Emily JoAnn Joyner is approved.

Guillaume Chanfreau

Harold G. Monbouquette

William M. Gelbart, Committee Chair

University of California, Los Angeles

2022

## **Dedication**

I dedicate this thesis to my family and friends, for their unwavering support.

## Table of Contents

Abstract of the Thesis .....	ii
The thesis of Emily JoAnn Joyner is approved .....	iv
Dedication .....	v
Table of Contents .....	vi
List of Figures, Tables, Symbols, Acronyms, Supplementary Materials, Glossary, etc. ....	viii
Acknowledgements .....	ix
CHAPTER 1 – Introduction .....	1
1.1 Introduction	
1.2 Description of Constructs	
CHAPTER 2 – Number of RNAs and Co-Transfections .....	9
2.1 Numbers of each RNA in transfections	
2.2 Transfection of BHK-21 cells	
2.3 Synthesis of Nodamura viral RNA constructs	
CHAPTER 3 – Fluorescent Protein Analysis .....	15
3.1 Introduction	
3.2 Methods	
3.3 Results	
CHAPTER 4 – RT-qPCR .....	22
4.1 Introduction	
4.2 Methods	
4.3 Results	
CHAPTER 5 – Conclusions and Discussion .....	32



5.1 Conclusions

5.2 Discussion

Works Cited .....36

## List of Figures, Tables, Symbols, Acronyms, Supplementary Materials, Glossary

Figure 1: Diagram of Nodamura Virus (NoV) replication and translation scheme .....	2
Figure 2: Schematics of viral RNA constructs .....	4
Figure 3: Three key transfection experiments .....	7
Equation 1: Calculation of the number of Nod1 EYFP RNA molecules added to transfection mix by mass .....	12
Equation 2: Calculation of the number of Nod2 mCherry RNA molecules added to transfection mix by mass .....	12
Figure 4: Representative brightfield and fluorescence images of cotransfected BHK-21 cells expressing both Nod1 EYFP and Nod2 mCherry RNAs, 24-hours post-transfection .....	18
Figure 5: Relative expression of Nod1 EYFP RNA over time post-transfection .....	19
Figure 6: Relative expression of Nod2 mCherry RNA over time post-transfection .....	20
Figure 7: Nod1 EYFP RNA standard curve for qPCR .....	25
Figure 8: Nod2 mCherry RNA standard curve for qPCR .....	26
Figure 9: qPCR numbers of Nodamura RNA molecules per cell from three key transfection experiments over time .....	27
Figure 10: Enhanced view of qPCR numbers of Nod2 mCherry RNA molecules per cell from transfection experiments over time .....	29
Figure 11: Enhanced view of qPCR numbers of Nodamura RNA molecules at early time points post-transfection .....	30

## **Acknowledgements**

I would like to thank Professor William Gelbart for his guidance and support during my time at UCLA. I would also like to thank Professor Emeritus Charles Knobler and everyone in the Gelbart/Knobler lab, all of whom have helped me get where I am today.

## Chapter 1: Introduction

### 1.1 Introduction

Viruses are obligate parasites that are entirely reliant upon successful entry into a host cell to multiply and begin their life cycle. Comprised of little more than a protein shell encapsulating genetic material, a virus must use the host's cellular machinery to express its proteins and generate many copies of itself. The focus of this study is the replication of viral genomes that take the form of positive-sense RNA – messenger RNA molecules that are directly translatable upon entering the host cell and being bound by a ribosome. As such, one of their gene products needs to encode the virus' genome replication enzyme, more specifically an RNA-dependent-RNA-polymerase (RdRp), that can bind and replicate the viral RNA genome. (Note that this enzyme is different from RNA-dependent-DNA-polymerase – “reverse transcriptase” – which *retroviruses* need to encode; in both cases – for positive-sense-RNA- and retro- viruses, the virus cannot depend on finding these enzymes in host cell.) RdRps are referred to as such because they must bind RNA to replicate it and generate a complementary daughter strand of RNA. In the case of positive-sense viruses, this first instance of replication generates a negative-sense strand that is complementary to the positive-sense RNA template from which it was replicated. Replication of this negative strand yields a daughter RNA in the positive sense, and repetition of this process ultimately generates large numbers of copies of the viral genome that can in turn be further replicated, translated, and – eventually – encapsidated to create viral progeny.

The experiments described in this study utilize the Nodamura virus as a model system to investigate *in cis* and *in trans* viral RNA replication. (The terms *in cis* and *in trans* will be defined in the next paragraph.) Nodamura has a single-stranded, positive sense genome

consisting of two RNA molecules. RNA1 encodes for the RNA-dependent RNA polymerase that binds and replicates both molecules of Nodamura's genome, while RNA2 codes for the capsid protein, which packages both molecules to form an infectious particle<sup>1</sup>. During its infection cycle, Nodamura RNA1 also produces a subgenomic RNA3 that through ribosomal frameshifting gives rise to two gene products, one of which is involved in suppressing host RNA interference and the other of which is of unknown function<sup>2</sup>. Because the in vitro studies described here are focused on the numbers of RNA1 and RNA2, with the aim of quantifying the competition between two molecules to be replicated by the same RdRp, we dispense with detection of RNA3.

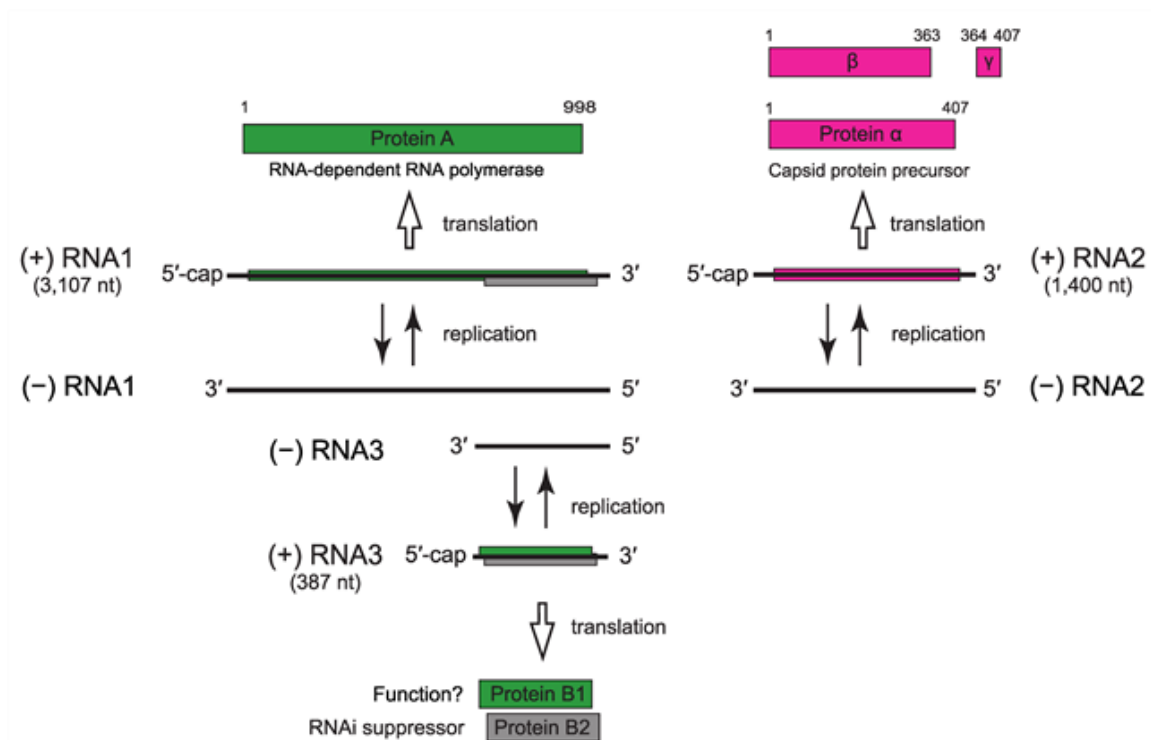


**Figure 1: Diagram of Nodamura Virus (NoV) replication and translation scheme<sup>3</sup>.** Diagram from Hameed et al.<sup>3</sup>; NoV RNA1 encodes the RdRp and the subgenomic RNA3, while RNA2 encodes the capsid protein.

The Nodamura virus (NoV) belongs to the *Nodaviridae* family of viruses, which includes two genera, *alphanodaviruses* and *betanodaviruses*<sup>1</sup>. In addition to Nodamura, other *alphanodaviruses* include Flock house virus (FHV) and Black beetle virus (BBV), all of which infect insects<sup>4</sup>. Nodamura, however, is unique in that it is also able to replicate in mammalian cells, including those of suckling pigs and mice<sup>5</sup>. Of particular interest to the present study, in vitro transcribed Nodamura virus RNA has previously been shown to successfully replicate in baby hamster kidney (BHK-21) cells upon transfection<sup>6</sup>.

An RNA molecule that encodes a protein that can bind and replicate the RNA from which it was translated is referred to as a *replicon*, and is said to undergo *in cis* replication. Conversely, an RNA molecule that is entirely dependent upon the protein product of a different RNA to be replicated is referred to as a *template*, and undergoes *in trans* replication. In the context of the Nodamura virus, RNA1, which encodes the RdRp, is replicated *in cis* and will be referred to as a *replicon*; RNA2, which relies upon being bound by the RdRp product of RNA1, is replicated *in trans* and will be referred to as a *template*. (RNA1 is *also* a template for the RdRp, but we will refer to it as the *replicon* and RNA2 as the *template*.)

As long as an RNA molecule contains the requisite 5' and 3' ends to be recognized and bound by the replication machinery, it can be replicated by the viral RdRp. Additionally, both Nodamura RNAs have 5' caps that enable them to be recognized and bound by the host cell's translational machinery, enabling expression of the viral proteins<sup>6</sup>. In the experiments performed in this study, Nodamura RNA1 and RNA2 molecules that contain different fluorescent reporter genes are

translated and replicated in BHK-21 cells, using fluorescence and RT-qPCR (reverse transcription quantitative polymerase chain reaction) assays to quantify their numbers.

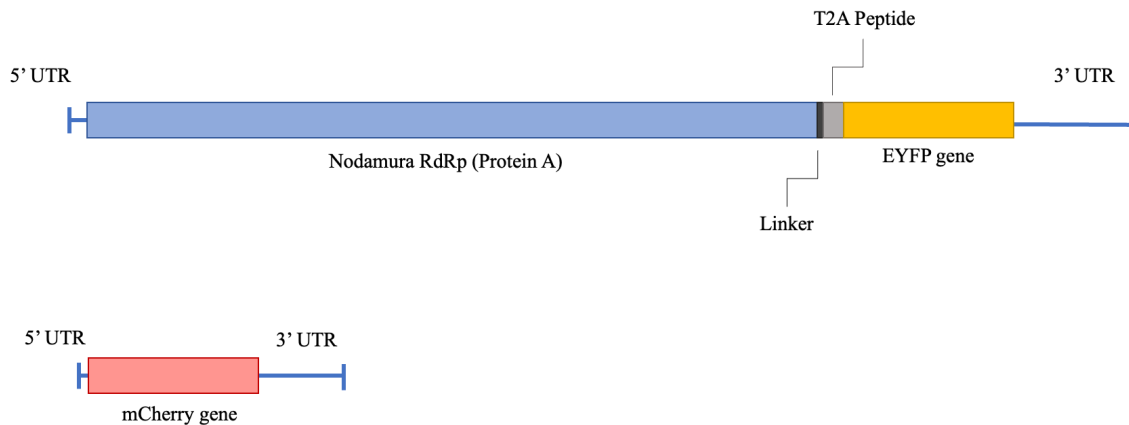


**Figure 2: Schematics of viral RNA constructs.** (A) Nodamura RNA1 EYFP construct, referred to as Nod1 EYFP. The RdRp ORF is indicated by the light blue box, the linker region by a black box, the T2A self-cleaving peptide sequence in grey, and the EYFP reporter gene in yellow. (B) Nodamura RNA2 mCherry construct, referred to as Nod2 mCherry. The capsid protein ORF has been replaced by the mCherry fluorescent protein gene. The Nodamura viral UTRs are indicated by the blue lines in both constructs. Both Nodamura RNA constructs are 5'-capped during *in vitro* transcription.

This phenomenon of *in cis* and *in trans* replication is fundamental to numerous other biological scenarios (in addition to many-molecule positive-sense-RNA-genome viruses like Nodamura) where several RNAs compete to be bound and replicated by a single replicase protein. For example, *defective interfering* RNAs, which are parasitic molecules that arise during the natural replication cycle of a virus because of errors in replication of the viral genome<sup>8</sup>. These defective RNA molecules no longer encode functional proteins, and yet are templates for the viral RdRp<sup>8</sup>.

They are referred to as interfering RNAs because they retain the necessary viral 5' and 3' UTRs and compete with the parent RNA to be bound and replicated by the replicase protein *in trans*, thereby lowering the level of replication of the functional viral genome.

Similarly, *in cis* and *in trans* replication underlies the working of viral *satellite-helper* systems. Tobacco mosaic virus (TMV) and satellite TMV (sTMV) are prime examples of this phenomenon. sTMV is a satellite virus, whose genome just encodes the capsid protein that packages and protects it, making it entirely dependent upon the RdRp of the 'helper' TMV virus to replicate its genome *in trans*<sup>9</sup>.

Finally, *superinfection exclusion* involves a primary infecting virus occluding a second, identical, virus from establishing a later infection in the same cell<sup>10</sup>. While each virus is functional and thus able to replicate itself *in cis*, they each in theory can undergo replication *in trans*, wherein the RdRp of the primary virus would bind and replicate the identical RNA genome of the secondary infecting virus. It has been shown that alphaviruses display superinfection exclusion, wherein replication of a secondarily infecting virus is almost entirely blocked by the presence of an existing viral infection in the cell, despite the two viruses being identical in every way except for the timing in which they entered the host cell<sup>10,11</sup>.

Elucidating the mechanics of *in cis* and *in trans* RNA replication during the viral infection cycle is not only key to understanding the nature of a virus's life cycle, but also has numerous translational medicine applications that feature defective-interfering RNA templates as antiviral agents that compete to be bound by viral RdRp against the viral genome, or that involve mRNAs



whose replication *in trans* would enhance the in situ synthesis of a therapeutic proteins. The present study utilizes fluorescent reporter assays and RT-qPCR to analyze and quantify *in cis* and *in trans* RNA replication behavior, using in vitro transcribed Nodamura virus RNA molecules that contain fluorescent reporters and are transfected into mammalian cells. Measuring fluorescent protein expression at various time points after transfection can be used as a proxy for studying relative replication levels of each RNA molecule present and can inform on the relative level of gene expression at that time. RT-qPCR, in contrast, provides a more explicit look at the actual numbers of RNA molecules present at that given time, and will be used similarly to track RNA replication and degradation behaviors post-transfection.

To assess *in cis* versus *in trans* RNA replication, this study uses three key transfection experiments. The first transfection involves a replicon RNA alone, which will inform on the baseline level of *in cis* replication this molecule undergoes in the absence of a competing molecule. The next transfection involves a template RNA alone, which – without the presence of an RdRp – is unable to replicate and amplify itself and can only be translated. Finally, the last experiment involves cotransfection of a replicon RNA and a template RNA. Amplification of the template RNA, observed using fluorescence quantification and RT-qPCR, compared to when it is transfected alone, will provide information about *in trans* RNA replication. Similarly, analyzing the levels of fluorescence and numbers of molecules of replicon generated, now in the presence of a competing template molecule, will provide insight about changes in *in cis* RNA replication occurring at various time points post-transfection.

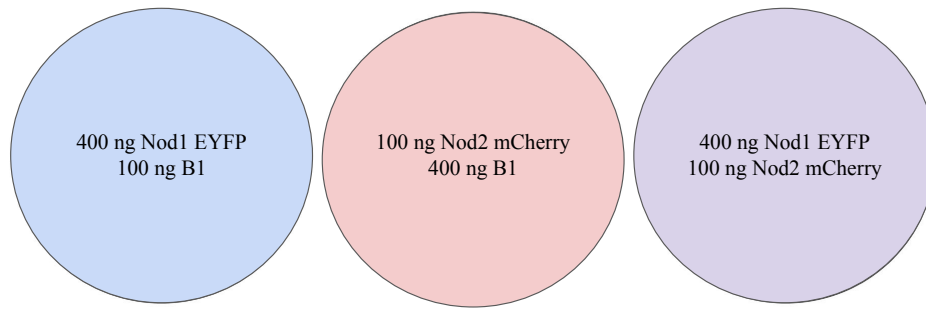


**Figure 3: Three key transfection experiments.** Equal *numbers* of Nod1 EYFP and Nod2 mCherry RNA are added in each experiment, by scaling the transfection-mix masses of each RNA by the ratio of their lengths. The first experiment involves transfection of Nod1 EYFP RNA ‘alone’ (blue circle), the second involves transfection of Nod2 mCherry ‘alone’ (red circle), and the final experiment involves cotransfection of both Nod1 EYFP and Nod2 mCherry RNAs (purple circle). In both ‘alone’ transfections, uncapped B1 RNA is added to satisfy the requirement for a fixed mass of RNA in the transfection mix.

## 1.2 Descriptions of Constructs

To probe *in cis* versus *in trans* RNA replication, several constructs were created using the Nodamura genomic RNA. The first construct is a version of Nodamura’s RNA 1, which encodes an open reading frame (ORF) for the RdRp protein (and the subgenomic RNA 3, which is not of interest here). A fluorescent reporter protein gene is added at the end of the RdRp ORF of RNA1, with a short linker sequence and a self-cleaving peptide (T2A) sequence between the end of the RdRp gene and the start of the reporter gene (Figure 1). Upon being bound by a ribosome, the entire molecule is translated from the RdRp start codon until the stop codon of the EYFP gene. However, the T2A peptide sequence induces ribosomal skipping during this translation, yielding two separate peptides: the functional RdRp protein (with the short linker sequence

added to its C-terminal end) and the EYFP reporter protein<sup>12</sup>. This RNA 1 reporter construct still retains its viral 5' untranslated region (UTR) and, following the end of the reporter gene, the viral 3' UTR, and as such is still able to be replicated by the viral RdRp. This particular fluorescent protein RNA 1 construct that has the gene for the Enhanced Yellow Fluorescent Protein (EYFP) appended to the end of the Nodamura RdRp ORF will be referred to as Nod1 EYFP Replicon.

The RNA 2-derived construct, in contrast, has the entire ORF for the capsid protein replaced by a reporter gene, while still retaining the viral 5' and 3' UTRs. The fluorescent reporter RNA 2 construct has the gene encoding the mCherry fluorescent protein, and will be referred to as Nod2 mCherry. Figure 1 shows diagrams and the names of these Nodamura RNA constructs. Nod1 EYFP is just over 4,200 nt in length, while Nod2 mCherry is approximately 1,000 nt in length.

## Chapter 2: Numbers of RNAs and Co-Transfections

### 2.1 Numbers of each RNA in transfections

Three key transfection experiments are performed in this study and are analyzed using fluorescence quantification and RT-qPCR methods: transfection of a replicon (Nod1 EYFP) RNA, transfection of a template (Nod2 mCherry) RNA, and the cotransfection of both molecules (Nod1 EYFP replicon and Nod2 mCherry template). However, to study *in cis* and *in trans* replication occurring in these three scenarios, it is important to start with the same *numbers* of each RNA molecule to be able to attribute changes in either fluorescence intensity or molecule counts to these replication phenomena; otherwise, any differences in fluorescence or molecule number could be due to differences in the initial molecule number transfected. Since the lengths of the two viral RNAs are not the same, different masses of each molecule are transfected, scaled by the ratio of their lengths, to ensure that equal *numbers* of each RNA are present in the transfection mixes.

A key assumption in analyzing these experiments is that efficiency of transfection is independent of the RNA-nucleotide sequence; if each of these RNAs involves roughly comparable numbers of each of the four nucleotides, then with few exceptions their amounts of secondary/tertiary structure and 3D sizes will be comparable enough to assume uniform lipoplex formation. (Note that these experiments deal with different RNA molecules that are each thousands of nucleotides long, rather than with short oligos: B1 RNA is about 3,200 nt, Nod1 EYFP is about 4,200 nt, and Nod2 mCherry is about 1,000 nt.) Across each transfection experiment, the total masses of both lipofectamine, the transfection agent, and RNA used are fixed. If these masses are both fixed, then regardless of transfection efficiency and composition of RNA present, the same amount of

RNA should be transfected into the cells in all of the experiments. To keep the total RNA mass consistent across the (replicon *or* template alone) single-RNA transfections and the (replicon *and* template) cotransfections, uncapped B1 RNA was used as an inert “filler” in the single-RNA experiments, to satisfy the constant total mass requirement. Since the total mass and the number of active RNAs (replicon and template) are the same in each transfection, the amount of RNA transfected into each cell should be identical. While the exact number of each RNA entering and being expressed in the cells is not known, it is only necessary that it be the same in each experiment.

More explicitly, suppose we want to cotransfect our two viral RNA molecules: Nod1 EYFP (~4,200 nt) and Nod2 mCherry (~1,000 nt). Since the mass of an RNA molecule is proportional to its nucleotide length, we can use the ratio of their lengths (~4:1) to determine the relative masses of each RNA we should add to ensure that equal numbers of both molecules are cotransfected. For a fixed total RNA mass of 500 ng per experiment, this ~4:1 length ratio works out to about 400 ng Nod1 EYFP RNA and 100 ng Nod2 mCherry RNA to be used for the cotransfection, with these masses equating to about  $\sim 1.8 \times 10^{11}$  molecules of each RNA in the transfection mix (Equations 1 and 2, below). As mentioned before, in addition to keeping the total RNA mass consistent across all experiments, we also want to keep the numbers of each viral RNA being transfected uniform in both the replicon or template alone transfections as well as in the cotransfection. Therefore, this same 400 ng mass of Nod1 EYFP RNA was used when this molecule was transfected ‘alone.’ To reach the required 500 ng total RNA mass (to ensure consistent transfection of RNAs across all experiments), 100 ng of the uncapped, “inert” B1 RNA was also added when assessing only Nod1 EYFP replication. Similarly, when transfecting

Nod2 mCherry ‘alone,’ 100 ng was used, in addition to 400 ng of the “inert” B1 RNA. As such, the same number,  $\sim 1.8 \times 10^{11}$  molecules, of each viral RNA was used in each of the three key transfection experiments.

The Brome Mosaic Virus RNA 1 (B1), used as an inert filler RNA to keep the total mass of RNA transfected the same in each experiment, is uncapped so that it will be minimally translated (if at all) in the cell and thus will not affect the replication and expression of the ‘active,’ capped viral RNAs<sup>13</sup>. Additionally, B1 RNA is similar enough in length to the other two Nodamura RNA constructs, to ensure that the lipoplexes that form around the RNA by the lipofectamine are as consistent in their properties as possible across all transfections<sup>13</sup>.

The experiments outlined here were performed in 24-well plates. Given that each well contains approximately  $1.9 \times 10^5$  cells at the time of transfection, and that there are approximately  $1.8-1.9 \times 10^{11}$  molecules of each Nodamura RNA construct in the transfection mix, the average number of RNA molecules of either kind transfected into a cell must be less than 1 million. These numbers will be measured using RT-qPCR.

$$\begin{aligned} \text{molecules Nod1 EYFP} &= \frac{4 \times 10^{-7} \text{ g Nod 1 EYFP}}{4,220 \text{ nt} \times \frac{321 \text{ g}}{\text{mol}}} \times \frac{6.02 \times 10^{23} \text{ molecules}}{\text{mol}} \\ &= 1.8 \times 10^{11} \text{ molecules Nod1 EYFP RNA} \end{aligned}$$

**Equation 1. Calculation of the number of Nod1 EYFP RNA molecules added to transfection mix by mass.** The number of molecules of Nod1 EYFP present in the transfection mix is dependent upon the initial mass of RNA added and the length of the RNA. 400 ng of the 4,220 nt-long Nod1 EYFP RNA was added in each transfection experiment. Here we have used 321g/mol as the average RNA nucleotide molecular weight.

$$\begin{aligned} \text{molecules Nod2 mCherry} &= \frac{1 \times 10^{-7} \text{ g Nod 2 mCherry}}{997 \text{ nt} \times \frac{321 \text{ g}}{\text{mol}}} \times \frac{6.02 \times 10^{23} \text{ molecules}}{\text{mol}} \\ &= 1.9 \times 10^{11} \text{ molecules Nod2 mCherry RNA} \end{aligned}$$

**Equation 2. Calculation of the number of Nod2 mCherry RNA molecules added to transfection mix by mass.** The number of molecules of Nod2 mCherry present in the transfection mix is dependent upon the initial mass of RNA added and the length of the RNA. 100 ng of the 997 nt-long Nod2 mCherry RNA was added in each transfection experiment.

## 2.2 Transfection of BHK-21 Cells

BHK-21 (baby hamster kidney) cells were seeded in 24-well plates and were transfected upon reaching 70 - 90% confluency. At total confluency, each well in the 24-well plate contains approximately  $0.24 \times 10^6$  cells. Thus, at the time of transfection (24 hours after seeding), each well contains approximately  $1.8\text{-}1.9 \times 10^5$  cells, or were about 80% confluent<sup>14</sup>. Lipofectamine 2000 reagent (Thermo Fisher) was diluted 1:10 in Opti-MEM Reduced Serum Medium (Thermo

Fisher). Cells were transfected using a volume of 5  $\mu$ L lipofectamine and a mass of 500 ng RNA per well, as specified by the manufacturer.

After adding the appropriate volumes of each RNA to reach a total mass of 0.5  $\mu$ g to be added per well, the volume of the mixture was brought up to 50  $\mu$ L, diluting with Opti-MEM medium. The RNA and Opti-MEM mixture were then combined with the diluted Lipofectamine, and incubated for 5 minutes at room temperature, to allow for incorporation of the RNA into the lipofectamine lipid complexes. After incubation, another 100  $\mu$ L of Opti-MEM was added to the mixture to bring the total volume of the transfection mixture to 200  $\mu$ L. The mixture was then added to each well of the 24-well plate, and this addition was designated as time 0 for the following transfection measurements.

### **2.3 Synthesis of Nodamura viral RNA constructs**

*Nod1 EYFP Replicon and Nod2 mCherry RNA:* The Nodamura RNA 1 construct used was derived from plasmids that were a generous gift from Dr. Leonid Gitlin in 2014, working at the time in Dr. Raul Andino's lab at UCSF<sup>15</sup>. The Nodamura RNA 2 construct was derived from plasmids created by Dr. Adam Biddlecome in the Gelbart lab<sup>15</sup>. Plasmids were linearized using XbaI restriction enzyme (New England BioLabs) and transcribed using the mMessage mMachinE T7 Transcription Kit (Thermo Fisher) to produce readily translatable, capped viral RNA. Manufacturers' protocols were followed for both procedures. Both RNAs were purified using a RNeasy Mini Kit (Qiagen), again following the manufacturer's specifications.

*B1 RNA:* Inert B1 RNA was in vitro transcribed from plasmid pT7B1 using a T7 Polymerase MegaScript kit (Thermo Fisher) after linearization with BamHI restriction enzyme (New



England BioLabs), following the manufacturers' protocols for both procedures. The MegaScript transcription kit yields uncapped RNA, which is ideal for generation of our inert, filler RNA B1, which should not be translated in cells for these experiments. Uncapped B1 RNA was purified using a RNeasy Mini Kit (Qiagen), again following the manufacturer's specifications.

## Chapter 3: Fluorescent Protein Analysis

### 3.1 Introduction

Insertion of fluorescent reporter genes into the viral genomes provides a simple and effective method to track and visualize viral replication in host cells<sup>16</sup>. In the case of the Nodamura RNA constructs used in this paper, insertion of fluorescent protein genes does not appear to have a drastic effect on either RNA's ability to be replicated *in vivo*, and readily enables detection of viral replication through fluorescence microscopy. The Nodamura RNA1 construct, which contains an EYFP reporter gene following the RdRp ORF, fluoresces a yellow-green color (excitation 513 nm, emission 527 nm), while the RNA2 mCherry construct fluoresces an orthogonal red color (excitation 587 nm, emission 610 nm), enabling simple distinction between their expressions in cotransfection experiments. Additionally, when using fluorescent quantification methods, such as a plate reader, the EYFP and mCherry proteins have different relative fluorescent intensity values (in relative fluorescent units, or RFU). As such, the maximum RFU values of either protein cannot be directly compared to one another. For the purposes of this study, we are only interested in comparing relative expression trends of each RNA to itself, and how that RNA's expression level changes over time, so this is not an issue in our analysis.

For fluorescence analysis of viral replication, several transfection experiments using the inert B1 and Nodamura RNA constructs were conducted. The first included cells that were transfected with just inert B1 RNA, serving as a transfection control. The next involved transfection of 'only' Nod1 EYFP replicon RNA, using inert B1 RNA to reach the total required RNA mass for transfection. Similarly, the next experiment included 'only' Nod2 mCherry template RNA with

inert B1 RNA. The final experiment involved the cotransfection of cells with equal *numbers* of both Nod1 EYFP replicon RNA and Nod2 mCherry template RNA. The same mass of any one viral RNA (ensuring the same *number* of each RNA) was added in both the cotransfection well and each RNA ‘alone’ well, as previously described. Each experiment was performed using biological duplicates, and fluorescence intensity values were measured in triplicate.

### **3.2 Methods**

#### *Harvesting cells*

Fluorescence intensity assay was performed, harvesting cells at the following time points post-transfection: 8, 18, 24, 48, 72 hours. The transfection mix was removed, cells were rinsed with Dulbecco’s Phosphate Buffered Saline (DPBS, Thermo Fisher), and media replaced with Dulbecco’s Modified Eagle Medium (DMEM, Thermo Fisher) at the 8-hour post-transfection time point. To obtain measurements at each time point, cells were rinsed with 0.5 mL DPBS and incubated with 100  $\mu$ L 0.25% Trypsin-EDTA (1X, Thermo Fisher) for 5 minutes. After incubation, 100  $\mu$ L DMEM with 1x penicillin/streptomycin and 10% Fetal Bovine Serum (FBS) (Thermo Fisher) were added to inactivate the trypsin.

Cells were then mixed using a micropipette, the total cell mixtures were transferred to Eppendorf tubes and spun for 5 minutes at 200 relative centrifugal force (rcf) to pellet the cells using a Thermo IEC MultiRF Tabletop Centrifuge. Once pelleted, the medium was aspirated off, and the pellet was resuspended in 200  $\mu$ L DPBS and transferred into 96-well microplates for fluorescence intensity measurements.

### *Fluorescence intensity measurements*

Fluorescent protein expression was measured in triplicate using a Molecular Devices SpectraMax® iD3 Multimode Microplate Reader. EYFP fluorescence was measured using an excitation wavelength of 513 nm and 553 nm emission. mCherry fluorescence was measured at an excitation wavelength of 587 nm and emission of 627 nm. Fluorescence microscopy images of BHK-21 cells expressing Nodamura viral RNAs were taken using an Amscope IN300TC-FL microscope at x20 magnification. Images were obtained using a 5-MP charge-coupled-device (CCD) camera and processed using TCCapture software. Brightfield images were taken at 200 ms exposure, while fluorescence images were captured using a 4.2 s exposure setting (Figure 3).

### **3.3 Results**

Nod1 EYFP expression levels, when transfected ‘alone,’ peaked between 24 and 48 hours, at approximately 1.2 million relative fluorescent units (RFU). Upon cotransfection, the expression of Nod1 EYFP decreased significantly when in the presence of Nod2 mCherry, only peaking at about 650,00 RFU (Figure 4). This suggests that Nod2 mCherry, which is a template, is now competing with RNA1 to be bound and replicated *in trans* by the RdRp, resulting in the apparent decrease in RNA1 levels in the cotransfection (dark blue curve) compared to when RNA1 was transfected alone (light blue curve). Keep in mind that the EYFP and mCherry fluorescent proteins intrinsically have different fluorescent intensities, and that we are interested in comparing *relative* changes in fluorescence of each protein to itself across the different experiments.

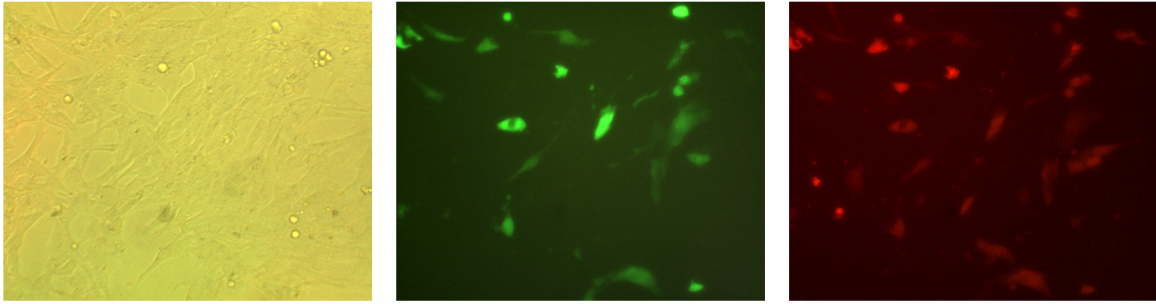


**Figure 4. Representative brightfield (left) and fluorescence images of cotransfected BHK-21 cells expressing both Nod1 EYFP (middle) and Nod2 mCherry (right) RNAs, 24-hours post-transfection.** Confirmation of co-transfection of both Nodamura viral RNA constructs and of fluorescent reporter protein expression in mammalian (BHK-21) cells.

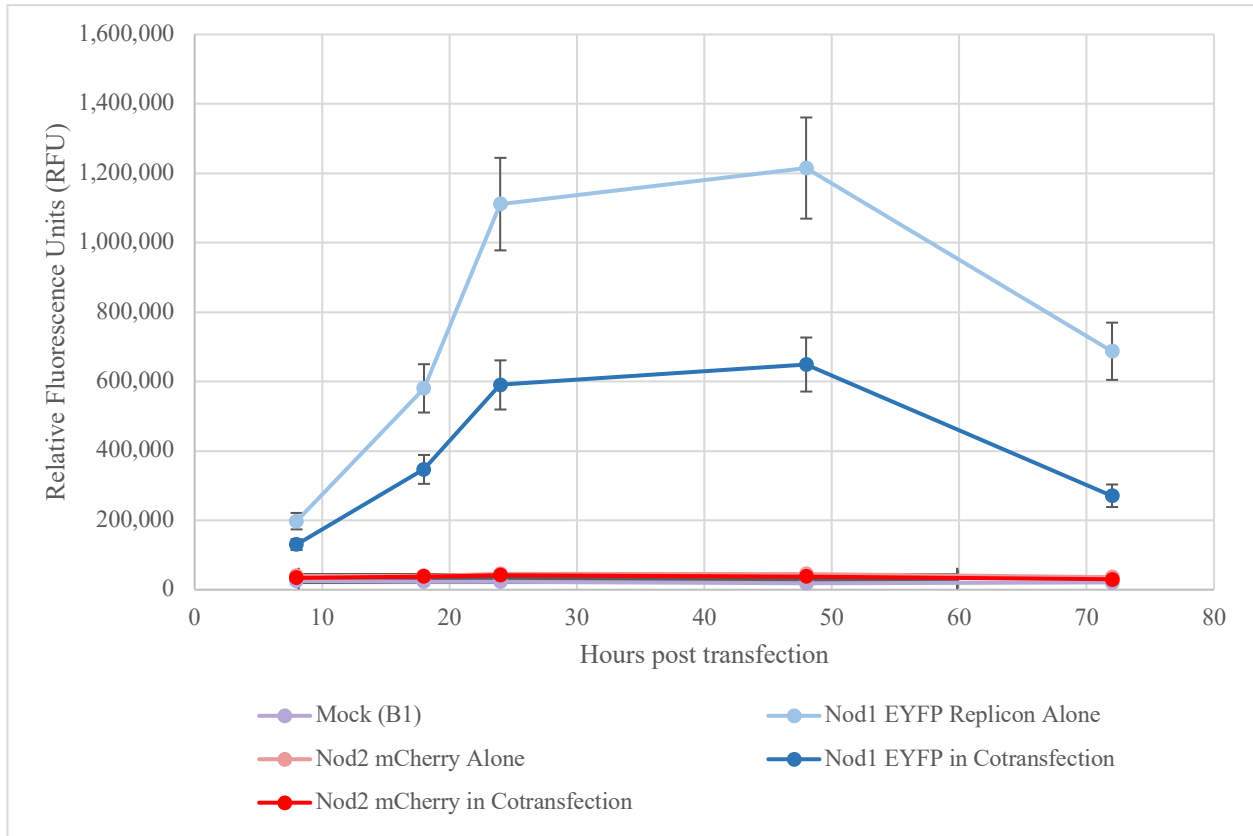


**Figure 5. Relative expression of Nod1 EYFP, Nod2 mCherry, and B1 alone RNAs over time post-transfection.** EYFP fluorescence expression levels, measured at 513 nm excitation and 553 nm emission, are indicated by the blue curves. The time course for Nod1 EYFP transfected alone is indicated by the light blue line, and that of Nod1 EYFP expression when cotransfected with Nod2 mCherry is indicated by the dark blue line. The “alone” and “co-transfected” time courses for Nod2 mCherry (see light and dark red) and for the control mock transfection using B1 RNA (see light purple) are presented on an amplified RFU scale in Figure 5. Error bars represent one standard deviation based on assay measurements taken in triplicate of biological duplicates.

Interestingly, the same time course for Nod2 mCherry revealed no significant amplification or expression of RNA2 throughout the course of the entire experiment. When Nod2 mCherry was transfected alone, its expression levels slightly peaked between 24 and 48 hours similarly to

RNA1, at approximately 46,000 RFU, suggesting this is when maximal translation of this RNA occurs (Figure 5). However, when Nod2 mCherry was cotransfected in the presence of Nod1 EYFP, its expression levels remained largely unchanged, and if anything decreased, peaking at about 42,000 RFU. This result is especially interesting, as the Nod1 EYFP data suggested that RNA1 is not being replicated at as high a level when in the presence of RNA2. Since the levels of Nod2 mCherry expression in the cotransfection never surpass that of the Nod2 mCherry alone experiment, it does not appear Nod2 mCherry is not being replicated *in trans* by the RdRp at all.

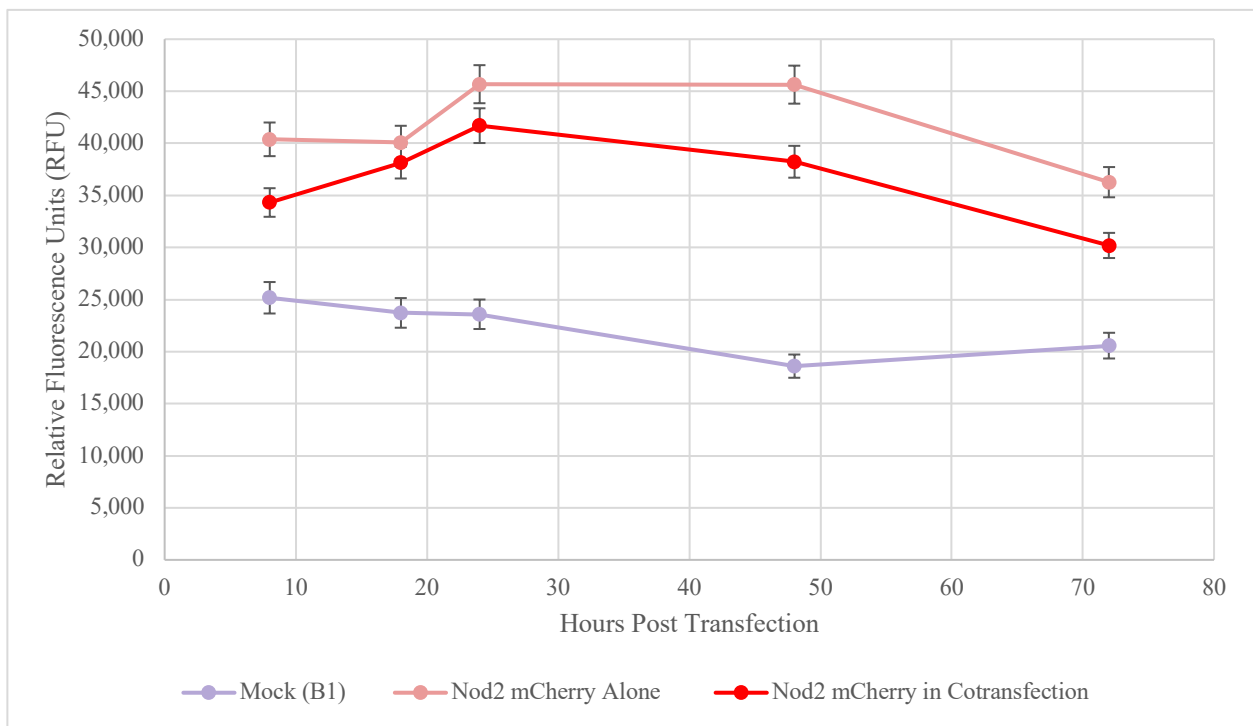


**Figure 6. Relative expression of Nod2 mCherry and B1 RNAs over time post-transfection.**

mCherry fluorescence expression levels, measured at 587 nm excitation and 627 nm emission, are indicated by the light and dark red curves. Time course of Nod2 mCherry transfected alone is indicated by the light red line, and that of Nod2 mCherry cotransfected with Nod1 EYFP is indicated by the dark red line. Control transfection of only B1 RNA is indicated by the light

purple line. Error bars represent one standard deviation based on assay measurements taken in triplicate of biological duplicates.

This data does not show any apparent amplification of RNA2, at least when measured by fluorescence. To further probe this result, RT-qPCR was performed to determine more accurate counts of each RNA molecule present throughout the time course, rather than relying upon downstream expression of reporter proteins to assess replication.



## **Chapter 4: RT-qPCR**

### **4.1 Introduction**

Quantitative polymerase chain reaction (qPCR) has been shown to be a powerful tool to study and quantify viral replication<sup>17</sup>. qPCR is an incredibly sensitive technique as it can enable detection of as few as ten copies of a nucleic acid transcript, making it perfect for studying viral replication in host cells, where an infection can be initiated from amplification of just one viral RNA molecule<sup>18</sup>. To study viral infection, PCR is often preceded by reverse transcription (RT), as many viruses have RNA genomes, which are not compatible with PCR and first must be converted to complementary DNA (cDNA). RT involves a reaction wherein RNA is combined with a reverse transcriptase enzyme, which generates a cDNA copy of the RNA of interest that is amenable for use in PCR<sup>19</sup>. For the experiments outlined in this study, our virus-derived RNAs – Nod1 EYFP replicon, and Nod2 mCherry – were purified from cells at various time points post-transfection and quantified using RT-qPCR. The *in vitro* transcribed RNA of both Nodamura constructs that were used to initially transfect were also used to generate standard curves used in the quantification of the viral RNAs harvested at each time point (Figures 6 and 7).

### **4.2 Methods**

#### *RNA purification*

RNA was purified for RT and qPCR at the following time points post-transfection: 1, 4, 8, 18, 24, and 48 hours. Transfection mix was removed, cells rinsed with 0.5 mL DPBS (Thermo Fisher), and medium replaced by 200  $\mu$ L DMEM (Thermo Fisher) at the 1-hour post-transfection time point. At each time point, cells were rinsed with 0.5 mL DPBS. After aspirating DPBS, 350  $\mu$ L Buffer RLT from RNeasy mini kit (Qiagen) was added to the cells and left to incubate for 1

minute. Cells were scraped off the plate using a pipette tip, resuspended in RLT, and transferred to an Eppendorf tube. The resuspension was added to a QiaShredder column (Qiagen), and spun at 10,000 x g for 1 minute. 350  $\mu$ L of 70% ethanol was added to the flow through from the QiaShredder column, and the entire mixture was moved to a RNeasy spin column. The manufacturer's protocol from the RNeasy mini kit (Qiagen) was followed for the rest of the RNA purification. Once purified, the RNA concentration at each time point sample was determined using a Nanodrop Spectrophotometer. The RNA purified at each time point was stored at -80°C until reverse transcription (RT) and qPCR were performed.

#### *Reverse Transcription*

The RNA purified as above from the transfections was reverse transcribed as follows. 1  $\mu$ g RNA was added to 1  $\mu$ L of reverse primer (100  $\mu$ M; against EYFP gene for Nod1 EYFP, or against mCherry gene for Nod2 mCherry), 1  $\mu$ L dNTPs (Deoxynucleotide (dNTP) Solution Mix, New England BioLabs, 10  $\mu$ M), and water. The mixture was then heated at 65 C for 5 minutes, then moved to ice for 5 minutes, and spun down. To this mixture, 2  $\mu$ L of 10x M-MuLV Reverse Transcriptase Buffer (New England BioLabs), 1  $\mu$ L M-MuLV Reverse Transcriptase enzyme (New England BioLabs), 0.2  $\mu$ L Protector RNase Inhibitor (Sigma Aldrich), and water were added to reach a total volume of 20  $\mu$ L. The tube was then spun down and the reaction was run at 42°C for 1 hour, then at 65°C for 20 minutes. The reaction tubes were then immediately placed on ice to cool, and this process was performed for each time point sample for each transfection experiment. For the cotransfection experiments, the RNA from the sample was used in two separate reactions: one using the Nod1 EYFP reverse primer (to generate cDNA of Nod1 EYFP

present in the sample) and the other reaction using Nod2 mCherry reverse primer (to generate cDNA of Nod2 mCherry present in the sample).

### *qPCR*

The standard curve method was employed to quantify the RNA purified from the transfection time courses, using in vitro transcribed Nod1 EYFP replicon RNA and Nod2 mCherry RNA to generate two standard curves that would be used to quantify the two different RNAs (Figures 6 and 7). The cDNA obtained from the previous RT step was diluted to create 1 ng and 100 pg samples. A qPCR reaction Master Mix was created by adding 10  $\mu$ L of the 2X SsoAdvanced Universal SYBR Green Supermix (Bio-Rad), 1  $\mu$ L of 10  $\mu$ M forward primer, 1  $\mu$ L of 10  $\mu$ M reverse primer, and 7  $\mu$ L water. 1  $\mu$ L of the 100 pg cDNA dilution was added to the Master Mix, which was then transferred to a 96-well qPCR plate. Each cDNA was measured in triplicate; therefore, three qPCR reactions were run per sample. qPCR was performed using a Bio-Rad CFX Connect Real-Time PCR Detection system using the following settings: enzyme activation step, 95°C, 30 seconds; annealing step, 95°C, 15 seconds; extension step, 60°C, 30 seconds; annealing and extension steps repeated for 40 cycles; melt curve, 65°C -90°C, increasing by 0.5°C per 5 minutes.

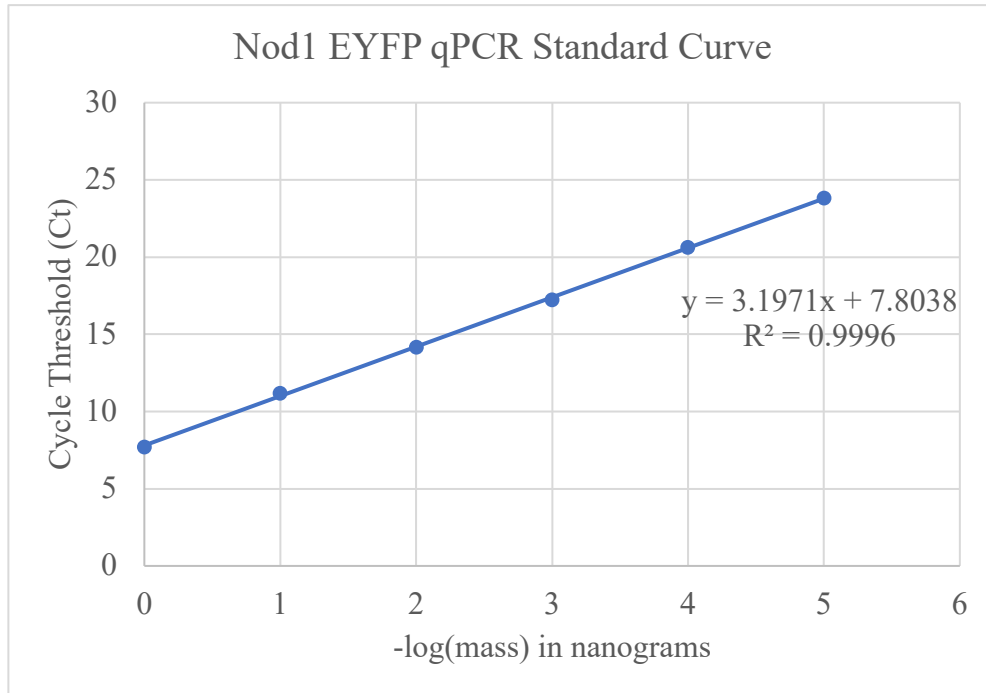


**Figure 7. Nod1 EYFP RNA standard curve for qPCR.** Standard curve was created using known dilutions of in vitro transcribed Nod1 EYFP replicon RNA for qPCR. The following dilutions of RNA were used to generate this standard curve: 1 ng, 100 (picogram) pg, 10 pg, 1 pg, 100 femtogram (fg), 10 fg.

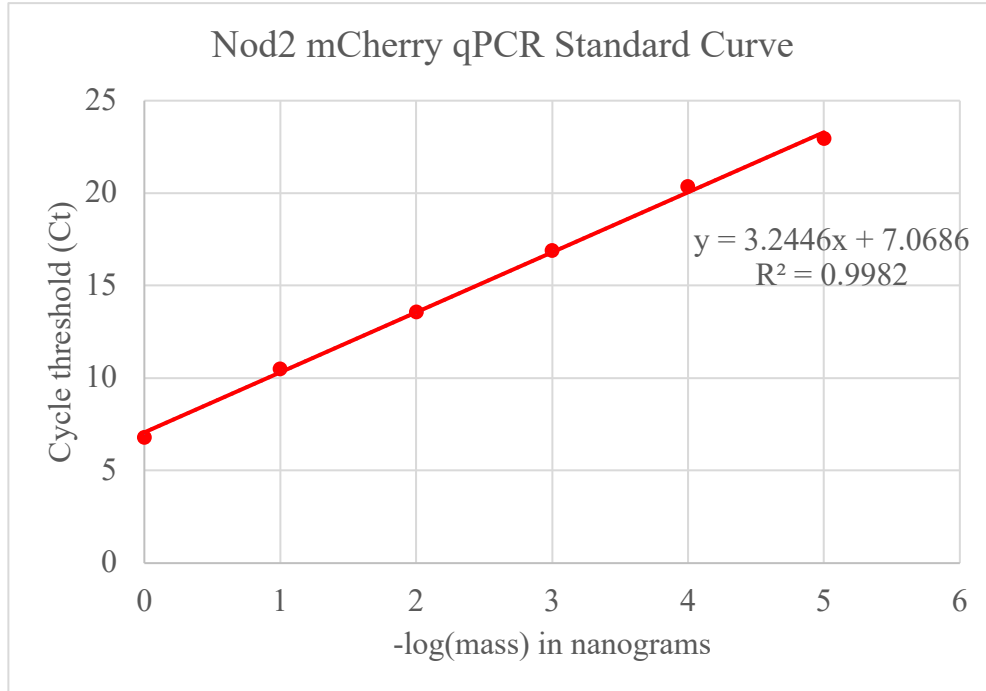


**Figure 8. Nod2 mCherry RNA standard curve for qPCR.** Standard curve was created using known dilutions of in vitro transcribed Nod2 mCherry RNA for qPCR. The following dilutions of RNA were used to generate this standard curve: 1 ng, 100 pg, 10 pg, 1 pg, 100 fg, 10 fg.

### 4.3 Results

The qPCR data indicates that 1 hour after initial transfection, immediately after the transfection mix is removed from the cells, approximately 200,000 molecules of each RNA construct per cell (out of a possible 1 million) had successfully been transfected and were able to be detected using qPCR. When transfected alone (*i.e.*, not in the presence of a competing template RNA molecule such as Nod2 mCherry), Nod1 EYFP replicon RNA levels peak around 18 hours post transfection at a value of about 5.5 million RNA molecules present per cell (Figure 8). Like the trend observed using the fluorescence intensity assay, the number of Nod1 EYFP replicon RNA molecules is 1.5 to 2 times lower in the cotransfection experiment (when both Nod1 EYFP replicon and Nod2 mCherry template are present, dark blue curve) compared to when Nod1

EYFP was transfected “alone” (with “inert” B1 RNA, light blue curve) (Figure 8). This trend, where the numbers of Nod1 EYFP RNAs peak before the numbers of EYFP fluorescent protein expression peak, is expected and further confirms this construct is behaving as expected. This suggests a decrease in *in cis* replication of Nod1 EYFP in the presence of the competing Nod2 mCherry template RNA.

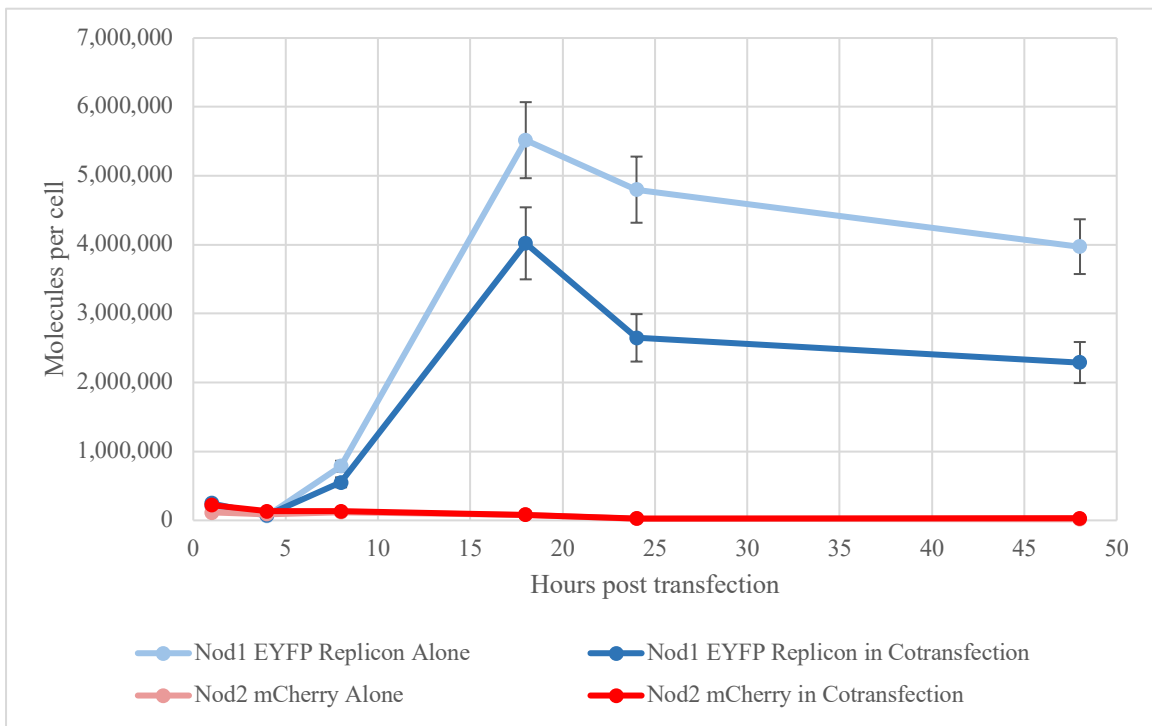


**Figure 9. qPCR numbers of Nodamura RNA molecules per cell from three key transfection experiments over time.** RNA was purified from cells at 1-, 4-, 8-, 18-, 24-, and 48-hours post-transfection, reverse transcribed, and quantified using qPCR. The number of molecules of Nod1 EYFP RNA per cell when transfected alone is indicated by light blue line; the number of Nod1 EYFP RNA molecules per cell when cotransfected is indicated by the dark blue line. The numbers of Nod2 mCherry in both the “alone” and cotransfection are indicated by the pink and

red lines respectively and are presented on an amplified RFU scale in Figure 9. Error bars represent one standard deviation from assay triplicate measurements.

qPCR analysis reveals that there is no significant amplification of Nod2 mCherry RNA in the cotransfection. The numbers of Nod2 mCherry RNA are a maximum at their initial 1-hour post transfection time point, at values near 150,000 molecules per cell (Figure 9), which further confirms the result seen in the fluorescence experiments. These results suggest that little, if any, *in trans* replication of Nod2 mCherry RNA is occurring in these cotransfection experiments, since the numbers of RNA2 molecules present in the cotransfection time course are not significantly different from Nod2 mCherry being transfected alone at any time point past 1-hour post transfection. This slightly higher number of Nod2 mCherry molecules present at early time points in the cotransfection time course compared to the Nod2 mCherry alone may just be due to experimental error and likely not a result of any replication of this molecule, since we do not see any *in cis* amplification of the replicon RNAs at this time. However, despite the initially different numbers of Nod2 mCherry RNAs, the numbers of Nod2 mCherry do not significantly vary from one another at any other time point except at 48-hours post transfection.

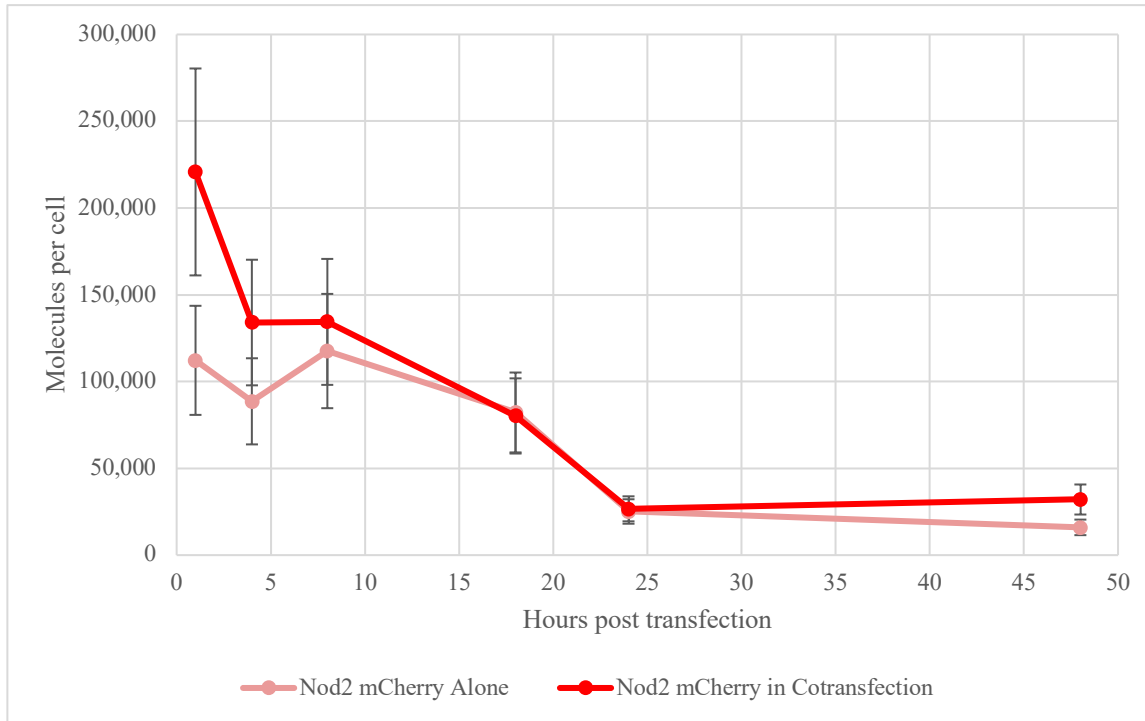


**Figure 10. Enhanced view of qPCR numbers of Nod2 mCherry RNA molecules per cell from transfection experiments over time.** RNA was purified from cells at 1-, 4-, 8-, 18-, 24-, and 48-hours post-transfection, reverse transcribed, and quantified using qPCR. The number of molecules of Nod2 mCherry RNA per cell when transfected alone is indicated by the light red line; the number of Nod2 mCherry RNA molecules per cell when cotransfected is indicated by the dark red line. Error bars represent one standard deviation from assay triplicate measurements.

Interestingly, it also appears that no significant replication of *any* RNA molecule is occurring before the 4-hour post transfection mark, as the numbers of the Nod1 EYFP replicon RNAs only begin to increase after this time point (Figure 10). Preceding this increase in replicon RNA numbers after the 4-hour post transfection time point there is a subtle decrease in the numbers of each RNA present compared to the initial number of molecules that were detected immediately post-transfection (1-hour time point). This is likely due to these foreign, viral RNAs being



degraded by the host cell before they can be sufficiently translated and replicated. Once enough replicon RNAs are translated, however, many RdRp molecules will be present in the cell and be able to amplify the replicon RNA.

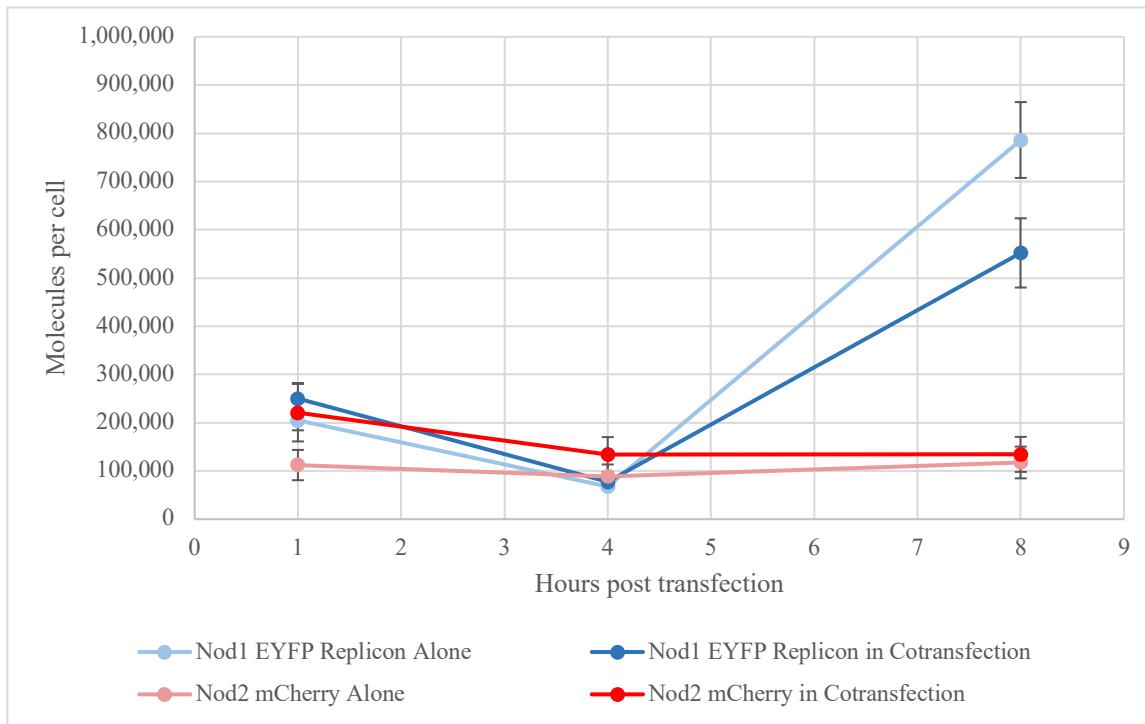


**Figure 11. Enhanced view of the qPCR numbers of Nodamura RNA molecules per cell at early time points post-transfection.** RNA was purified from cells at 1-, 4-, and 8-hours post-transfection, reverse transcribed, and quantified using qPCR. 1-hour post-transfection, approximately 200,000 molecules of each RNA molecule successfully enter the cells and are detected using qPCR. The levels of RNA decrease between 1 and 4 hours, but evidence of *in cis* RNA replication becomes clear between 4- and 8- hours post-transfection. Error bars represent one standard deviation from assay triplicate measurements.

This qPCR data confirms that Nod1 EYFP is less efficiently replicated by its RdRp when in the presence of Nod2 mCherry, and that Nod2 mCherry is not being significantly amplified in the cotransfection experiment (Figures 8-10). Additionally, this data also suggest that replication and amplification of the viral RNA does not increase until after 4 hours, and that the primary phenomenon occurring immediately post-transfection is likely translation of the viral RNAs. Once sufficient numbers of the RdRp are translated, there is a sharp increase in the numbers of RNA molecules as they are amplified by the replicase.

## Chapter 5: Conclusions and Discussion

### 5.1 Conclusions

While viral replication has been previously studied in numerous specific contexts, little work has focused directly on the general phenomenon of *in cis* versus *in trans* RNA replication in relation to the viral life cycle. The present study has analyzed *in cis* and *in trans* RNA replication in the context of the Nodamura virus, whose genome consists of RNA1 encoding its RdRp and RNA2 encoding its capsid protein. For this study, EYFP has been inserted into the 3' end of the RdRp ORF as a fluorescent reporter, while the capsid protein of RNA2 has been entirely replaced with the mCherry fluorescent protein gene. These two *in vitro* transcribed mRNA constructs were transfected into mammalian cells, using both fluorescent quantification of the protein reporters and qPCR to quantify the numbers of these RNAs as a function of time as part of three key transfection experiments. The first experiment involved transfection of 'only' the Nod1 EYFP replicon RNA, and the next experiment involved transfection of 'only' the Nod2 mCherry template RNA. (Here 'only' is put in quotes because Nod1 and Nod2 are actually *cotransfected* with an inert/noncompetitive RNA to ensure that equal numbers of the two molecules are transfected.) The final experiment entailed *cotransfecting* both the Nod1 EYFP replicon and Nod2 mCherry template RNAs, in equal numbers.

Both the fluorescence intensity and qPCR assays revealed that Nod1 EYFP RNA is replicated at a lower level when in the presence of a competing template RNA, namely Nod2 mCherry, compared to when it is transfected alone (i.e., with the inert RNA, B1). When only the Nod1 EYFP replicon RNA is expressed, both its reporter protein and numbers of RNA peak dramatically starting about 1-day post-transfection, indicating significant *in cis* replication

(Figures 4 and 8). In the presence of the competing Nod2 mCherry template RNA, however, Nod1 EYFP reporter protein expression decreases as much as two-fold (Figure 4), and the numbers of amplified replicon RNA decrease by nearly 1.5-fold (Figure 8). While this would suggest that the RdRp is likely also binding and replicating RNA2 *in trans*, the results presented here indicate that little amplification of Nod2 mCherry is actually occurring (Figure 9). Nod2 mCherry RNA did not show significant amplification in terms of numbers of RNAs present or reporter protein expression when cotransfected with the Nod1 EYFP replicon RNA, as demonstrated by the unchanging expression of its reporter protein and of the numbers of Nod2 mCherry RNA present throughout the cotransfection time course (Figures 5 and 9). While significant levels of *in cis* replication were anticipated to be observed in these experiments, the near complete lack of *in trans* replication of RNA2 was quite surprising.

This data also provided interesting insights into transfection efficiency and early viral replication dynamics post-transfection. Specifically, qPCR revealed that for each RNA – when the transfection mix contains enough RNA to transfect about one million molecules of each RNA per cell – approximately 200,000 molecules are successfully transfected and detected at 1 hour immediately after removing the transfection mix (Figure 10). This finding, that approximately the same numbers of RNA1 and RNA2 are transfected per cell, confirms our previously stated assumption that if the RNA molecules are similar enough in length and nucleotide composition they should have similar lipofectamine transfection efficiencies. Additionally, early qPCR time points reveal that between 1- and 4- hours post-transfection there is no viral RNA amplification occurring (Figure 10). During this time, it is likely that the RNAs are largely being bound by host cell ribosomes and translated. However, between 4- and 8- hours post-transfection there is a

significant spike in Nod1 EYFP replicon RNA numbers, indicating that *in cis* replication is occurring. It also becomes apparent that even during this early replication period, the difference in replication between Nod1 EYFP transfected ‘alone’ versus its replication in the presence of a competing Nod2 mCherry template RNA is notable. And, as previously mentioned, despite the obvious *in cis* replication occurring at these early time points and the discrepancy between Nod1 EYFP RNA numbers when transfected alone and in the cotransfection, there is no apparent *in trans* amplification of Nod2 mCherry RNA. It could be that RdRps are simply binding to Nod2 templates, and not replicating them, and yet being sequestered by Nod2 so as to decrease the availability of RdRps for binding *and replicating* Nod1 molecules.

## 5.2 Discussion

The results of this study are especially interesting, as early work investigating Nodamura virus replication by Ball et al. has shown that RNA2 undergoes notable amplification 5- and 22-hours post-transfection<sup>6</sup>. The discrepancy between the results found in the present study and this earlier work requires further investigation. One key difference between these studies is that Ball et al. used NoV viral RNA derived from a vaccinia virus vector system that is transfected into BHK-21 and later harvested for analysis. As such, the NoV RNAs used in the Ball study contain unperturbed viral genes, which more closely mimics wild-type viral replication. The present study uses *in vitro* transcribed RNAs that contain reporter proteins: in the case of RNA1, EYFP has been inserted into the 3’ end of the RdRp ORF, disrupting the production of the subgenomic RNA3, while RNA2’s capsid protein ORF has been completely replaced by the mCherry gene. It is important to mention the potential role that these structural proteins and the products of the subgenomic RNA3 may play in establishing and sustaining viral infection. As such, the RNAs

used in the experiments described in this study provide an important but limited perspective on the behaviors of wild-type Nodamura RNAs and their replication behaviors in mammalian cells.

Future experiments will be performed to repeat the qPCR experiments to accumulate more data points and replicates to further confirm the lack of RNA2 amplification seen in this system.

Additionally, the fluorescent protein assays will be repeated – not only to further confirm the results presented here, but also – to obtain earlier time points to compare relative levels of RNA translation occurring early post-transfection, similar to what was obtained for the qPCR data.

Another interesting iteration of these experiments would involve scaling the transfection mix to use less viral replicon RNA, as the current 400 ng of self-amplifying Nod1 EYFP RNA may be overwhelming the cells, resulting in the unexpected replication behavior observed here.

Nevertheless, this study has established a solid foundation for future experiments to probe *in cis* and *in trans* viral RNA replication using this simple two-molecule viral genome.

## Works Cited

- (1) Ball, L.A., Johnson, K.L. (1998). Nodaviruses of Insects. In: Miller, L.K., Ball, L.A. (eds) *The Insect Viruses. The Viruses*. Springer, Boston, MA.  
[https://doi.org/10.1007/978-1-4615-5341-0\\_8](https://doi.org/10.1007/978-1-4615-5341-0_8).
- (2) Gitlin L, Hagai T, LaBarbera A, Solovey M, Andino R. 2014. Rapid evolution of virus sequences in intrinsically disordered protein regions. *PLoS Pathog* 10:e1004529.  
<https://doi.org/10.1371/journal.ppat.1004529>.
- (3) Sahul Hameed, A. S., Ninawe, A. S., Nakai, T., Chi, S. C., & Johnson, K. L. (2019). ICTV Virus Taxonomy Profile: Nodaviridae. *Journal of General Virology*, 100(1), 3–4.  
<https://doi.org/10.1099/jgv.0.001170>.
- (4) Johnson, K. L., Price, B. D., and Ball, L. A. (2003). Recovery of Infectivity from cDNA Clones of Nodamura Virus and Identification of Small Nonstructural Proteins. *Virology*, 305(2), 436–451. <https://doi.org/10.1006/viro.2002.1769>.
- (5) Garzon, S., and G. Charpentier. 1991. Nodaviridae, p. 351–370. In J. R. Adams and J. R. Bonami (ed.), *Atlas of invertebrate viruses*. CRC Press, Boca Raton, Fla.
- (6) Ball, L. A., Amann, J. M., & Garrett, B. K. (1992). Replication of Nodamura virus after transfection of viral RNA into mammalian cells in culture. *Journal of virology*, 66(4), 2326–2334. <https://doi.org/10.1128/JVI.66.4.2326-2334.1992>.

- (7) Dasmahapatra, B., Dasgupta, R., Ghosh, A., & Kaesberg, P. (1985). Structure of the black beetle virus genome and its functional implications. *Journal of Molecular Biology*, 182(2), 183–189. [https://doi.org/10.1016/0022-2836\(85\)90337-7](https://doi.org/10.1016/0022-2836(85)90337-7).
- (8) Pathak, K. B., & Nagy, P. D. (2009). Defective Interfering RNAs: Foes of Viruses and Friends of Virologists. *Viruses*, 1(3), 895–919. <https://doi.org/10.3390/v1030895>.
- (9) Mirkov TE, Mathews DM, Du Plessis DH, Dodds JA. Nucleotide sequence and translation of satellite tobacco mosaic virus RNA. *Virology*. 1989 May;170(1):139-46. doi: 10.1016/0042-6822(89)90361-9. PMID: 2718378.
- (10) Adams, R. H., & Brown, D. T. (1985). BHK cells expressing Sindbis virus-induced homologous interference allow the translation of nonstructural genes of superinfecting virus. *Journal of virology*, 54(2), 351–357. <https://doi.org/10.1128/JVI.54.2.351-357.1985>
- (11) Singer ZS, Ambrose PM, Danino T, Rice CM. Quantitative measurements of early alphaviral replication dynamics in single cells reveals the basis for superinfection exclusion. *Cell Syst*. 2021 Mar 17;12(3):210-219.e3. doi: 10.1016/j.cels.2020.12.005. Epub 2021 Jan 29. PMID: 33515490.



- (12) Liu, Z., Chen, O., Wall, J., Zheng, M., Zhou, Y., Wang, L., Vaseghi, H. R., Qian, L., & Liu, J. (2017). Systematic comparison of 2A peptides for cloning multi-genes in a polycistronic vector. *Scientific reports*, 7(1), 2193. <https://doi.org/10.1038/s41598-017-02460-2>
- (13) Tanimoto, C. R., Thurm, A. R., Brandt, D. S., Knobler, C. M., & Gelbart, W. M. (2022). The nonmonotonic dose dependence of protein expression in cells transfected with self-amplifying RNA. *Journal of Virology*, 96(7). <https://doi.org/10.1128/jvi.01858-21>.
- (14) Thermo Fisher Scientific. (n.d.). *Useful numbers for cell culture*. Thermo Fisher Scientific - US. Retrieved April 12, 2022, from <https://www.thermofisher.com/us/en/home/references/gibco-cell-culture-basics/cell-culture-protocols/cell-culture-useful-numbers.html>.
- (15) Biddlecome, A., Habte, H. H., McGrath, K. M., Sambanthamoorthy, S., Wurm, M., Sykora, M. M., Knobler, C. M., Lorenz, I. C., Lasaro, M., Elbers, K., & Gelbart, W. M. (2019). Delivery of self-amplifying RNA vaccines in in vitro reconstituted virus-like particles. *PloS one*, 14(6), e0215031. <https://doi.org/10.1371/journal.pone.0215031>.
- (16) Li, Y., Li, L. F., Yu, S., Wang, X., Zhang, L., Yu, J., Xie, L., Li, W., Ali, R., & Qiu, H. J. (2016). Applications of Replicating-Competent Reporter-Expressing Viruses in Diagnostic and Molecular Virology. *Viruses*, 8(5), 127. <https://doi.org/10.3390/v8050127>.

- (17) Watzinger, F., Ebner, K., & Lion, T. (2006). Detection and monitoring of virus infections by real-time PCR. *Molecular aspects of medicine*, 27(2-3), 254–298.  
<https://doi.org/10.1016/j.mam.2005.12.001>.
- (18) Emery, S. L., Erdman, D. D., Bowen, M. D., Newton, B. R., Winchell, J. M., Meyer, R. F., Tong, S., Cook, B. T., Holloway, B. P., McCaustland, K. A., Rota, P. A., Bankamp, B., Lowe, L. E., Ksiazek, T. G., Bellini, W. J., & Anderson, L. J. (2004). Real-time reverse transcription-polymerase chain reaction assay for SARS-associated coronavirus. *Emerging infectious diseases*, 10(2), 311–316. <https://doi.org/10.3201/eid1002.030759>.
- (19) Farkas, D. H., Holland, C. A. (2009). Overview of molecular diagnostic techniques and Instrumentation. *Cell and Tissue Based Molecular Pathology*, 19–32.  
<https://doi.org/10.1016/b978-044306901-7.50008-0>.